ADVANCES IN FOREST FIRE RESEARCH

2022

Edited by
DOMINGOS XAVIER VIEGAS
LUÍS MÁRIO RIBEIRO

Physics-Based Modelling for Mapping Firebrand Flux and Heat Load on Structures in the Wildland-Urban Interface

Amila Wickramasinghe[1]; Nazmul Khan[1]; Alexander Filkov[2], Khalid Moinuddin[1]

[1]Institute for Sustainable Industries and Liveable Cities, Victoria University, Melbourne, VIC 3030, Australia {p.wickramasinghe@live.vu.edu.au; {Nazmul.khan, Khalid.Moinuddin}@vu.edu.au
[2] School of Ecosystem and Forest Sciences, Faculty of Science, University of Melbourne, VIC 3363, Australia, {alexander.filkov@unimelb.edu.au}

**Corresponding author*

Keywords

Physics-based modelling, firebrands, wildland fire, bushfire attack level, AS3959

Abstract

The mechanisms of wildfire attack on structures are classified into direct flame contact, radiant heat, firebrand attack and a combination of two or all of them. Arguably, airborne firebrands play a vital role as one of the main causes of structure ignition and fire propagation by forming spot fires far from the fire front. Firebrand flux (the number of firebrands landed on a unit area per unit time) and the heat load are important parameters to calculate the wildfire risk on structures. Australian Building Standard AS3959 is developed based on radiation heat flux and it does not quantify the effects of firebrand flux on structures to assess the wildfire risk completely. To improve the assessment of the Bushfire Attack Level (BAL) in AS3959, there is a need for the quantification of firebrand flux at different scales of wildfires. Lacking information about firebrand generation from various vegetation species under different environmental conditions creates a gap to estimate the firebrand flux accurately. In this study, we aim to use a physics-based model to quantify the firebrand generation rate of Eucalyptus dominant forest vegetation at different severities of wildfires expressed by the Fire danger indices (FDI) of 100, 80, and 50. The wind speed was chosen while keeping the temperature, relative humidity, and drought factor as constants to obtain the focused FDIs. A 40 m height Eucalyptus forest was modelled with 25 t/ha understorey and 10 t/ha canopy fuel loads as per AS3959 forest vegetation classification. The forest fires were prescribed with the intensities of 53.4, 43.1, and 27 MW/m with 100 m length to replicate the fire events explained by FDIs. The depth of the fireline was approximated according to the fire residence time and the spread rate. The firebrand size, shape, and quantity were taken from our previous firebrand generation study (Wickramasinghe et al. 2022) and the particles were injected randomly through the forest volume which is engulfed by the fire. The distances between the modelled structure that follows an Australian standard house design and the vegetation were maintained according to the BALs. We obtained the radiative heat flux on the houses close to the algorithm provided in AS3959 for each BAL. In this study, both firebrand and heat flux were quantified at strategic locations of the house. We find a logarithmic relationship exists between firebrand flux and radiative heat flux in the range of R2 0.96 to 0.99. Hence, for a certain BAL, the firebrand flux increases with the FDI similar to radiative heat flux. Results from this study can be used to quantify the firebrand flux on various house patterns from different vegetation fires, which may improve the design standards and construction requirements of buildings to mitigate the vulnerability of houses at the wildland-urban interface (WUI).

1. Introduction

Firebrand generation from burning vegetation is a potential threat to people and infrastructure in the wildland-urban interface due to the unpredictable nature of spotting[1]. This phenomenon can be severe with the scale of the wildfire and structural ignition becomes harder to control. Postfire investigations reveal more than 50% of houses destroyed by the wildfires are from firebrands and 2/3 of homes ignited directly or indirectly by the wind

[1] The phenomenon of ignition and starting a new fire front by burning material like wood chips, bark, twigs, leaves, or nuts ahead of the central fire front.

dispersed firebrands (Maranghides & Mell, 2011). Leonard et al.(2004) claim firebrands caused the ignition of over 90% of houses in Australia during a number of wildfire events.

The firebrand generation has received the least attention compared to the latter three aspects of the key processes of firebrand studies: transport, spotting, and secondary ignition. It is difficult to build an integrated system to replicate a realistic wildfire scenario and quantify the risk without adequate knowledge of firebrand generation. Safety issues, the need for advanced instruments, and large financial and human resources to measure firebrand generation at the fire front make the quantification of firebrand generation more difficult. However, physics-based modelling is identified as a viable alternative to finding the firebrand generation associated with the influence of vegetation species and different environmental conditions. Some physics-based models show the capability of predicting firebrand transport and short-range spotting through validation processes (Wadhwani et al., 2017). The validation of physical models requires thermophysical properties of vegetation, characteristics of firebrands including shapes, size, number, the intensity of the fire, the environmental conditions such as wind, fuel moisture content (FMC), and relative humidity, temperature etc. Various bench-scale and field-scale experiments have been conducted to understand the importance of these parameters to use in physics-based models.

Collecting firebrands from tree torching and management scale fires is a widely used technique to investigate the morphologies, characteristics and landing distribution of firebrands. The effects of vegetation species, fuel load, FMC, and wind speed are examined to understand the firebrand generation and their ignition propensity. Manzello et al.(2007) , Hudson et al.(2020) and Adusumilli et al.(2021) found firebrand collection significantly increases with the decrement of FMC. Most of the vegetation species investigated by Bahrani et al.(2020) show the number of firebrands collection increase with the wind speed. The parametric studies conducted through physics-based models by Thurston et al.(2017), Bhutia et al.(2010), and Tse et al.(1998) conclude the significance of firebrand characteristics, wind speed, and intensity of the fire for spotting. The relationship between fire intensity and the firebrand flux was firstly investigated by Thomas et al.(2017) through a prescribed forest fire experiment. With these experimental data of Thomas et al.(2017) the firebrand generation of a Pitch Pine forest was estimated through physics-based modelling by Wickramasinghe et al.(2022) using an inverse analysis technique. This modelling maintains fire intensities, wind climate, fuel properties, and firebrand characteristics (shape, size, composition) to replicate the field experiment and found the firebrand generation rate as 4.18 pcs/MW/s (pcs: pieces).

To the best of the authors' knowledge, there is no standard document that provides quantitative information about firebrand flux on structures in the WUI. Having a substantial understanding of firebrands flux is important to establish building standards to mitigate the wildfire risk with fidelity. Australian standard AS3959 – the prescription for constructing buildings in wildfire-prone areas – qualitatively presents the increment of firebrand attack with the radiative heat flux. The radiative heat flux is expressed in terms of Bush fire Attack Level (BAL) which describes the safe distance to the structure from the edge of the vegetation.

In the present work, we conduct a series of physics-based simulations to quantify the firebrand flux on structures incorporated with the radiative heat flux given in AS3959 for forest vegetation classification. As firebrand attack is the main cause of house ignition during wildfires in Australia, including quantified firebrand flux correlated to the current radiative heat flux is important to implement the BAL of AS3959 standard to better counter the wildfire risk on houses in WUI.

2. Methodology

The simulations are conducted using a physics-based model Fire Dynamic Simulator (FDS) (McGrattan et al., 2005) which is a product of National Standards Technology, USA. FDS uses the multiphase modelling technique, and the gas phase is simulated by Large Eddy Simulation (LES), while the solid firebrands are introduced in the domain by Lagrangian particle-based transport scheme.

2.1. Firebrand generation rate calibration for vegetation species, wind, and FMC

The firebrand generation rate (4.18 pcs/MW/s) found for Pitch Pine at 31% FMC and 2 m/s wind speed (Wickramasinghe et al., 2022) is used as the base information for calibration of the firebrand generation rate for Eucalyptus. The Eucalyptus and Pitch pine vegetations are relatively similar species in terms of the average tree

height, crown shape, orientation of leaves etc. Due to the scarcity of data, we assume the firebrand generation rate of Eucalyptus is the same as the Pitch pine at the same wind speed and FMC. Therefore the numerical effect of vegetation species in between these two fuels for firebrand generation could be approximated as 1:1. To calibrate the effect of wind speed for firebrand generation of Eucalyptus, we use the experimental data of Barani et al.(2020) obtained for the Loblolly Pine at different wind speeds. The physical appearance of Loblolly Pine and Eucalyptus are similar to use in the analysis. It shows increasing wind speed results in a higher number of firebrand production. Based on these experimental data, we obtain the mathematical relationship as presented in equations 1(a) and 1(b), for the number of generated firebrands against the wind speed to estimate the firebrand generation number at the wind speeds for FDI 100, 80, and 50:

$$fb_{generation} = 33.39 \times U_{wind} + 202.03 \;\; when \; 0 < U_{wind} < 8.19 \; ms^{-1} \quad 1(a)$$

$$fb_{generation} = 575 \;\; when \; 8.19 \; ms^{-1} \; < U_{wind} \quad 1(b)$$

where $fb_{generation}$ is the number of firebrand generation and U_{wind} is the wind speed at the burning vegetation. The firebrand generation ratio is calculated in reference to the number of firebrands generated at 2 m/s as shown in Table 1.

Table 1: Firebrand generation ratio according to the wind conditions for FDIs 50, 80, and 100.

Similar vegetations	Firebrand generation rate (pcs/MW/s)	Wind speed (m/s)	Number of firebrands	Generation ratio to 2 m/s
Loblolly Pine	4.18	2.00 (reference)	298	(298/298)=1.00
		5.48 (FDI 50)	454	(454/298)=1.52
Eucalyptus	(Pitch Pine at 2 m/s)	8.88 (FDI 80)	575	(575/298)=1.93
		10.38 (FDI 100)	575	(575/298)=1.93

The effect of FMC is evaluated as per Hudson et al.(2020) where higher FMC is associated with a lower number of firebrand production. Ponderosa Pine is the matching vegetation species to Eucalyptus in this tree burning experiments and the relationship between firebrand production and FMC is mathematically derived as presented in equation (2):

$$fb_{generation} = -4.7 \times FMC + 538.32 \quad (2)$$

where FMC is the dry basis fuel moisture content. By that, the firebrand generation ratio of Eucalyptus is estimated reference to the 31% of FMC as shown in Table 2.

Table 2: Firebrand generation ratio according to the FMC for FDIs 50, 80, and 100.

Similar vegetations	Firebrand generation rate (pcs/MW/s)	FMC (%)	Number of firebrands	Generation ratio to 3.84% FMC
Ponderosa Pine	4.18	31 (reference)	393	(393/393)=1.00
Eucalyptus	(Pitch Pine at 31%)	3.84 (all FDIs)	520	(520/393)=1.33

The final firebrand generation rates are approximated by the multiplication of the quantified individual generation ratios of species, wind, and FMC with the reference firebrand generation rate of Pitch Pine. Hence, the firebrand generation rates of forest vegetation for FDI 50, 80, and 100 are found as 8.43, 10.68, and 10.68 pcs/MW/s to use as inputs in the FDS model.

2.2. Model set up

The simulation domain size is chosen as 336 m× 102 m × 90 m with a 1.5 m grid size at the wind developing region and 0.75 m grid size at the area where fireline, firebrand generation and landing occur. These grid sizes are determined according to the grid convergence analysis of Wickramasinghe et al.(2022). Fig. 1 illustrates the developed wind flow introduced with eddies as per Jarrin et al.(2006), prescribed fire, fire-induced buoyancy, and the firebrand landing on the modelled house.

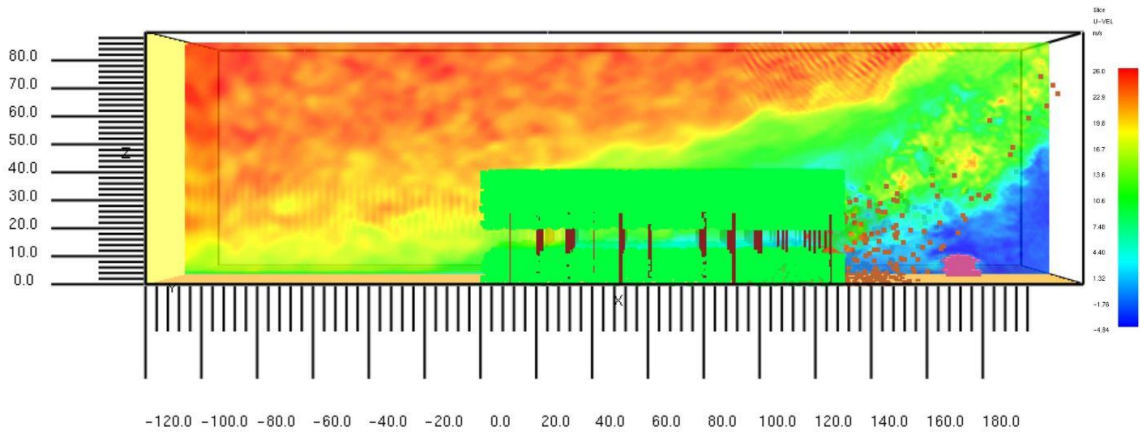

Figure 1- A Smokeview (the visual companion software of FDS) representation of the simulation of Forest fire at FDI 100 and BAL 12.5. The distance between the house and the forest edge is maintained as 50 m according to the BAL.

15 simulations were conducted varying the three different FDIs and five different BALs to calculate the firebrand flux and heat load on the house. The firebrand flux was measured at the strategic locations (gutter, deck, roof, window corners, sub-floor) of the house where firebrands can accumulate and start a secondary ignition. The radiative heat flux was also recorded at the same locations. The total firebrand flux is calculated based on the total number of firebrands received on a unit area of the house at a unit time. The maximum radiative heat flux is taken as the highest value obtained by a heat flux device at any strategic location. We plot the total firebrand flux against the radiative heat flux for FDIs as shown in Fig. 2. Each data point is related to a BAL (or the location of the house downwind).

3. Results and discussion

We use the maximum radiative heat flux and the total firebrand flux on the house to develop a mathematical correlation. According to Fig. 2, the firebrand flux on the house shows a logarithmic relationship with the radiative heat flux with an R^2 of 0.96, 0.98 and 0.99 for FDI 100, 80, and 50 respectively. Both FDI 100 and 80 curves are located over FDI 50 implying the higher firebrand risk for the same radiative heat flux. Although the curves are quite close for the lower three BALs, the FDI 100 has positioned above the FDIs 80 and 50 after BAL 29. This indicates that the firebrand attack is higher for FDI 100 than the FDIs 80 and for some BALs when the house is located close to the fireline.

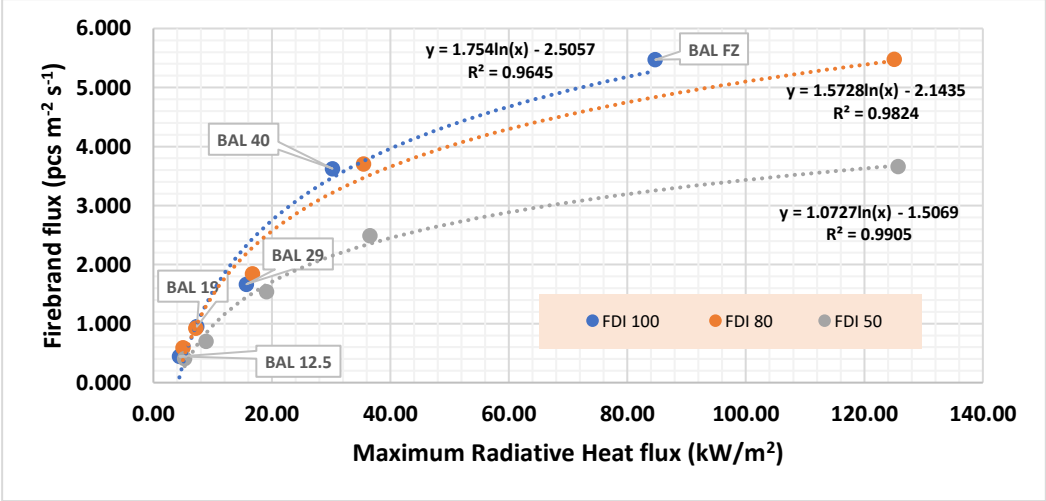

Figure 2- The correlation of the firebrand flux and the radiative heat flux for forest vegetation at FDI 100, 80, and 50.

4. Conclusion

A series of physics-based simulations have been conducted to quantify the firebrand flux on a structure located in the downwind direction of a burning forest. The influences of vegetation species, wind speed, and FMC were calibrated to find the resultant firebrand generation rate to use as inputs in the Eucalyptus tree burning model. The thermophysical data were taken from the literature and the model was set up according to the fuel loads, FDIs, and BALs as given in the AS3959 standard. The firebrand flux and the radiative heat flux on the house were calculated and found a logarithmic relationship between the two parameters. The quantification of firebrand attack was correlated with the existing radiative heat flux to improve the building construction requirements of AS3959 to mitigate the wildfire risk on buildings in the WUI.

5. References

Adusumilli, S., Hudson, T., Gardner, N., & Blunck, D. L. (2021). Quantifying production of hot firebrands using a fire-resistant fabric. International Journal of Wildland Fire, 30(2), 154-159.

Bahrani, B. (2020). Characterization of Firebrands Generated from Selected Vegetative Fuels in Wildland Fires The University of North Carolina at Charlotte].

Bhutia, S., Ann Jenkins, M., & Sun, R. (2010). Comparison of firebrand propagation prediction by a plume model and a coupled–fire/atmosphere large–eddy simulator. Journal of Advances in Modeling Earth Systems, 2(1).

Hudson, T. R., Bray, R. B., Blunck, D. L., Page, W., & Butler, B. (2020). Effects of fuel morphology on ember generation characteristics at the tree scale. International Journal of Wildland Fire, 29(11), 1042-1051.

Jarrin, N., Benhamadouche, S., Laurence, D., & Prosser, R. (2006). A synthetic-eddy-method for generating inflow conditions for large-eddy simulations. International Journal of Heat and Fluid Flow, 27(4), 585-593.

Leonard, J., Blanchi, R., & Bowditch, P. (2004). Bushfire impact from a house's perspective. Earth Wind and Fire–Bushfire 2004 Conference, Adelaide,

Manzello, S. L., Maranghides, A., & Mell, W. E. (2007). Firebrand generation from burning vegetation. International Journal of Wildland Fire, 16(4), 458-462.

Maranghides, A., & Mell, W. (2011). A case study of a community affected by the Witch and Guejito wildland fires. Fire technology, 47(2), 379-420.

McGrattan, K. B., Forney, G. P., Floyd, J., Hostikka, S., & Prasad, K. (2005). Fire dynamics simulator (Version 5): User's guide. US Department of Commerce, Technology Administration, National Institute of Standards and Technology.

Thomas, J. C., Mueller, E. V., Santamaria, S., Gallagher, M., El Houssami, M., Filkov, A., Clark, K., Skowronski, N., Hadden, R. M., & Mell, W. (2017). Investigation of firebrand generation from an experimental fire: Development of a reliable data collection methodology. Fire Safety Journal, 91, 864-871.

Thurston, W., Tory, K. J., Fawcett, R. J., & Kepert, J. D. (2017). Long-range spotting by bushfire plumes: The effects of plume dynamics and turbulence on firebrand trajectory.

Tse, S. D., & Fernandez-Pello, A. C. (1998). On the flight paths of metal particles and embers generated by power lines in high winds-a potential source of wildland fires. Fire Safety Journal, 30(4), 333-356.

Wadhwani, R., Sutherland, D., Ooi, A., Moinuddin, K., & Thorpe, G. (2017). Verification of a Lagrangian particle model for short-range firebrand transport. Fire Safety Journal, 91, 776-783.

Wickramasinghe, A., Khan, N., & Moinuddin, K. (2022). Determining firebrand generation rate using physics-based modelling from experimental studies through inverse analysis. Fire, 5(1), 6.